

Scatter Radiation Absorbed Dose Distribution in Coronary Angiography: A Measurement-Based Study

Seyed Abdolhamid Talebi¹, Salman Jafari^{2*}, Reza Afzalipour^{3,4}, Faraj Tabeie⁵, Seyed Pejman Shirmardi⁶

1. Department of Medical Physics, School of Medicine, Tehran University of Medical Sciences, Tehran, Iran.
2. Department of Radiology, Faculty of Paramedicine, Hamadan University of Medical Sciences, Hamadan, Iran.
3. Department of Radiology, Faculty of Paramedicine, Hormozgan University of Medical Sciences, Bandar Abbas, Iran
4. Molecular Medicine Research Center, Hormozgan Health Institute, Hormozgan University of Medical Sciences, Bandar Abbas, Iran
5. Department of Basic Sciences, School of Rehabilitation Sciences, Shahid Beheshti University of Medical Sciences, Tehran, Iran
6. Nuclear Science Research School, Science Research School, Nuclear Science & Technology Research Institute (NSTRI), Atomic Energy Organization of Iran, Tehran, Iran

ARTICLE INFO

Article type:
Original Paper

Article history:

Received: Jul 10, 2021
Accepted: Nov 04, 2021

Keywords:

Angiography
Radiation Dosages
Radiation Dosimeter
Fluoroscopy

ABSTRACT

Introduction: This study aimed to investigate the absorbed dose of scatter radiation in coronary angiography.

Material and Methods: The scatter radiation dose was measured for 20 patients at four different heights (50, 100, 150, and 165 cm) from the floor. The spatial dose was measured by RTI Piranha r100b solid-state dose probe at different points around the patient in an actual clinical situation and with a phantom. Also, the measurement was repeated using a designed phantom in fluoroscopy and cine mode in posterior anterior (PA), left lateral (LLAT), left posterior oblique (LPO45°), right posterior oblique (RPO45°), and right-lateral (RLAT) projections. Organ-absorbed doses were normalized to dose area product (DAP).

Results: The dose rate at different heights between the projections on the patient and the phantom as well as organ dose DAP conversion coefficients were different ($p < 0.05$). It was found that the dose rate changes in fluoroscopic mode compared to cine mode are significantly different ($p = 0.001$). The dose rate in cine mode is approximately four times that in fluoroscopy mode. The dose rate around the cardiologist's waist could be reduced by 37 – 43 % with a displacement of 20cm away. In this study, the effective dose rate received by the cardiologist's eyes was higher than those reported by ICRP.

Conclusion: Taking a suitable projection could reduce the dose rate delivered to the angiography team. Further studies should be conducted about the effect of different projections with the same clinical use on dose distribution in coronary angiography to provide the best working conditions for physicians and staff.

► Please cite this article as:

Talebi SA, Jafari S, Afzalipour R, Tabeie F, Shirmardi SP. Scatter Radiation Absorbed Dose Distribution in Coronary Angiography: A Measurement-Based Study. Iran J Med Phys 2022; 19: 250-257. 10.22038/IJMP.2021.58875.1986.

Introduction

Cardiovascular diseases are the leading cause of death worldwide [1,2]. Based on the world health organization fact sheet, the world's biggest killer is ischemic heart disease, responsible for 16% of the world's total deaths [3]. Obstruction of coronary arteries restricts the blood flow to the myocardium and causes ischemia. Accurate diagnosis of obstruction is important, and different imaging modalities, including angiography, CT angiography, and nuclear medicine are common methods used for this purpose. Among these methods, angiography is considered the gold standard [4-7]. One of the concerns about CT and angiography is the carcinogenic effects of low-dose scattered radiation in these modalities [8, 9]. Despite advances in technology, angiography is still an invasive method for patients, and cardiologists and other persons involved in the procedure have to stand beside the patient while working [10]. One thing to worry about is the

absorbed dose to them because of scattered radiation from the patient's body and other instruments on the way of the primary beam [2, 11]. The maximum tube kilovoltage and exposure time of angiography are higher than radiography, resulting in higher scattered radiation [12- 14]. In order to reduce the exposure, solutions such as image receptors with higher detecting quantum efficiency and conversion factor and under-table tube configuration have been utilized, but there is still a concern about low dose radiation [15-17]. Given the high dose rate in angiography (600-1200 $\mu\text{Sv}/\text{min}$) compared to radiography (1-10 $\mu\text{Sv}/\text{min}$) radiation, protection principles including keeping a distance from the source as far as possible, low exposure time, and shield become more critical [13, 14]. In addition, monitoring the absorbed dose to cardiologist and other personnel is necessary. Usually, personal dosimeters such as film badges are used for this purpose. It is a common approach among

*Corresponding Author: Tel: +98-813-838-1043; Email: salman.jafari21@gmail.com

angiography centers, but the number and location of dosimeters on the body may differ [18, 19]. Placing the dosimeters on the lead cover results in an overestimate of the dose, making it necessary to use correction factors for cover attenuation. On the other hand, under the lead cover, the dose rate is relatively low which in turn causes uncertainty in the dose reading [20]. Spatial dose distribution around the patient as a scatter source, and angiography equipment depends on different factors such as the arrangement of the devices, room geometry, patient size, and imaging projection [21]. Awareness of the dose distribution can help cardiologists choose a low-risk location, beware of high-risk areas, and put their film badges in a suitable place. In this study, we examined the dose distribution around the patient and phantom using a solid-state dosimeter.

Materials and Methods

This study was performed using a digital angiography system AXIOM Artis dFc made by Siemens. It is equipped with the automatic exposure control system (AEC), which could set exposure parameters kVp, and mAs and add or remove extra filtration, i.e., filters with thicknesses 0.1, 0.2, 0.3, 0.6, and 0.9 mm copper. The X ray tube position was under the table but there was no lead curtain. Two mode imaging of fluoroscopy and cine-fluorography was possible with 10, 15 and 30 pulses per second (PPS). The spatial dose was measured by RTI Piranha r100b solid-state dose probe at different points around the patient in an actual clinical situation and with a phantom. For former, all patients (n=20) were lying on the bed in a supine position and angiography was performed in a posterior-anterior (PA) projection. Exposure parameters were selected automatically by the AEC system. To avoid disturbing the work of the cardiologist a symmetric location at the opposite side was determined for dosimeter. The measurement set up is shown schematically in figure 1.

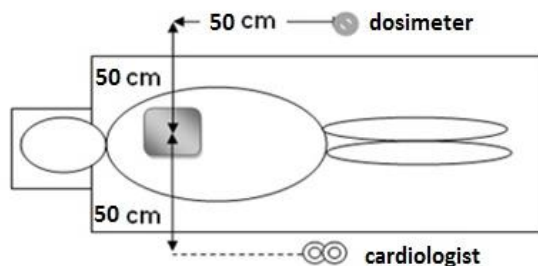


Figure 1. Patient position and location of cardiologist and dosimeter for spatial dose measurement in actual angiography conditions.

Dosimeter is fixed at a distance of 50 cm away from central ray in four points 50, 100, 150, and 165 cm height from the floor. For each point, the measurement repeated four times and the average of them was considered as absorbed dose. To investigate more about the absorbed dose around angiography device for other

patient position and projections additional measurements were performed using phantom. A water phantom (ISO design) with dimensions of $30 \times 30 \times 15$ cm³ was made of poly methyl methacrylate (PMMA) which wall thickness was 1 cm (figure 2).

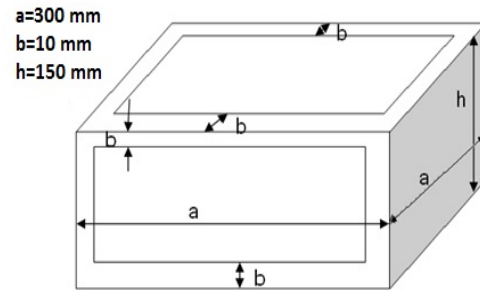


Figure 2. Schematic view of the designed phantom for this study

This phantom was located under beam to simulate the patient during irradiation. In this case, measurements were performed in more projections; i.e., PA, left posterior oblique (LPO45°), right posterior oblique (RPO45°), right-lateral (RLAT), and left lateral (LLAT). In PA projection, spatial dose was measured at distances of 50 and 75 cm from the center of the bed at heights of 100, 150, and 165 cm from the floor. To investigate the dose distribution in the direction of the bed, the location of the cardiologist was considered as a reference, and the dosimeter moved each time a distance of 20 cm longitudinally. This was done at a height 100 cm from the floor and a distance 50 cm from the bed center, as shown in figure 3.

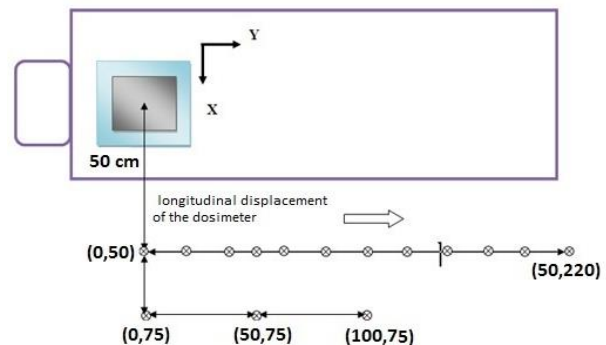


Figure 3. Schematic representation of longitudinal dose distribution measuring with phantom for projection PA.

DAP for each projection was obtained from the console. Then measured absorbed doses in organs were normalized to DAP to provide the DAP-to-dose conversion coefficients.

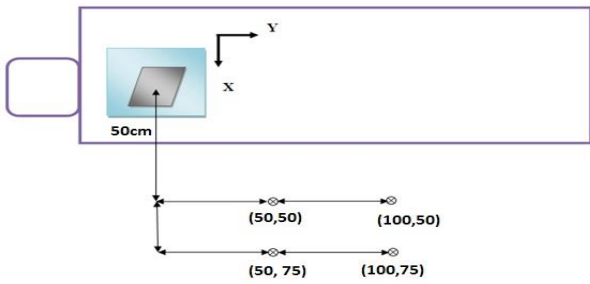


Figure 4. Schematic representation from longitudinal dose distribution measuring with phantom for other projections.

Also, measurement was performed at distance of 75 from the center of the bed with replacement of 50 cm longitudinally. Measurement coordinates for other projections are shown in figure 4. Kruskal-Wallis test was used to compare dose rate values at different altitudes. Dose rate changes in cine and fluoroscopy modes were statistically analyzed using T-Test and a p-value less than 0.05 was considered statistically significant.

Results

Absorbed dose rate measured at a distance of 50 cm away from central ray in four points 50, 100, 150, and 165 cm height from the floor in actual angiography condition are given in table 1. These points are the alignment of the knee, waist, thyroid, and eyes for a person of average height. All patients (n=20) were in supine position, and angiography was performed in PA projection. Kruskal-Wallis test showed a significant difference (P = 0.05) in dose rate values at different altitudes. Dose rate variations along the longitudinal direction were checked out with phantom instead of patient, and the results are shown in figure 5.

Dose rate changes in cine and fluoroscopy modes were statistically analyzed using a T-Test. It was found that the dose rate changes in fluoroscopic mode compared to cine mode are significantly different (p = 0.001). The dose rate in cine mode is approximately four times that in fluoroscopy mode. Also, the dose rate variations between points spaced 20 cm apart in each mode were examined by the ANOVA test, and there was a significant difference (P = 0.05). By increasing the distance from the tube toward the patient's foot, the average dose can be reduced to 1.43 and 1.37 times in cine and fluoroscopy mode, respectively.

Table1. Absorbed dose rate in actual angiography condition and PA projection

Patient number	Weight(kg)	Age(year)	Organ Dose Rate[μ Gy/h]			
			50 cm	100 cm	150 cm	165 cm
1			-	-	126.66	100.33
2			1337	1039	404.55	348.66
3			906	310.3	132.6	59.66
4			-	703	-	-
5	Not available	Not available	241	213.33	1283.66	2031.33
6			-	491	-	-
7			-	286	-	-
8			-	-	289.66	271.33
9			-	662	-	-
10	85	69	2096.3	895	175.33	145
11	78	64	1030	680	375.3	-
12	59	65	-	362	207	-
13	76	41	-	-	125	73
14	70	56	1206	373.66	188	134.3
15	73	58	1568.7	642.6	256.6	-
16	75	-	1998.7	0	466.3	152.3
17	83	48	-	1344.7	432.7	173.7
18	54	-	-	1344.7	371.6	97.3
19	65	56	-	-	-	152.3
20	85	75	2258.7	1781	440.7	237.7
		mean	1603.6	829.5	280.4	156.3
		STDV	507	444	124.2	82.6

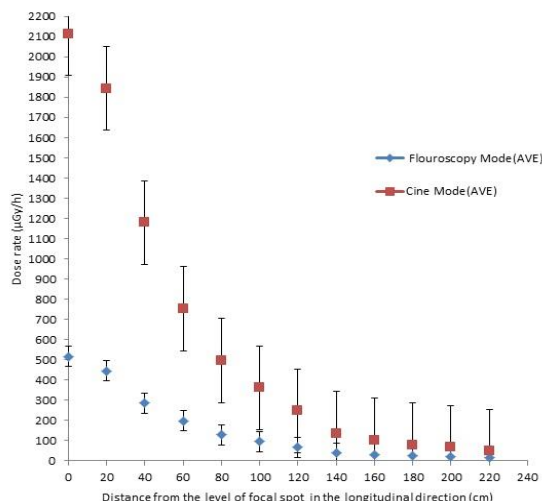


Figure 5. Dose rate variations along the longitudinal direction at the height of 100 cm from the floor and 50cm distance from bed center.

Table 2. Dose to DAP conversion rates for actual angiography conditions

Patient no	DAP Rate (Gy. m ² /h)	Oragan Dose/DAP[µGy/Gy.cm ²]			
		knee	waist	neck	eyes
1	0.74	--	--	1.71	1.35
2	2.34	5.71	4.42	1.72	1.48
3	1.66	5.44	1.86	0.79	0.35
4	8.39	--	0.83	--	--
5	2.37	1.10	0.89	5.4	8.55
6	6.26	--	0.87	--	--
7	5.92	--	0.82	--	--
8	3.33	--	--	0.86	0.81
9	6.59	--	1	--	--
10	2.99	6.99	2.98	0.58	0.48
11	12.47	0.82	0.54	0.30	--
14	11.17	1.07	0.33	0.16	0.12
15	1.69	9.24	3.78	1.51	--
16	1.97	10.11	5.43	2.35	0.77
18	5.37	--	2.49	0.69	0.18
19	3.24	6.95	5.48	1.35	0.73

Table 3. Vertical dose rate variations at the location of the cardiologist

Height(cm)	X and Y	Cine mode (µGy/hour)			Fluoro mode [µGy/hour]		
		100(cm)	50(cm)	0(cm)	100(cm)	50(cm)	0(cm)
h=100	50	362	1183.3	2114.8	95.5	286.25	517.25
	75	140	346.75	360.75	37	89.75	111.5
h=150	50	313.25	361.5	695	92.25	115.25	177.5
	75	265.75	393.5	597.25	75.5	103.25	152.25
h=165	50	263.5	294	273.5	66.5	76	66.75
	75	226.5	297.25	403.25	64.75	83.25	100

Table 4. Dose rate measurements in 4 projections of LLAT, RLAT, LPO45 ° and RPO45 ° in two fluoroscopy and cine modes

Projection	Height(cm)	X and Y	cine mode[$\mu\text{Gy}/\text{hour}$]		fluoro mode[$\mu\text{Gy}/\text{hour}$]	
			100(cm)	50(cm)	100(cm)	50(cm)
RLAT	h=100	50	144.25	555.5	47	144.75
		75	119	135.5	31	23.25
	h=150	50	266.5	579.75	92.25	151
		75	205.25	335	63.25	113.25
	h=165	50	247.5	403.25	37.5	107.25
		75	232	395.75	67.5	105.5
RPO45°	h=100	50	244	1489.5	72.75	907.5
		75	182.25	346.25	53.25	86.5
	h=150	50	884.75	1513.5	253.25	427.5
		75	662.25	1002	186.5	278
	h=165	50	841.5	1114.75	226.25	316.5
		75	751.75	771.75	190.5	215.75
LPO45°	h=100	50	5664.25	5402	1734.5	1275.25
		75	1826.75	7638.25	414.25	1753.75
	h=150	50	1763.25	3405.75	505	960.25
		75	1610	3078.25	483.25	803.5
	h=165	50	1574.75	2169	465.75	647.5
		75	1544.25	2306.5	418.75	362.5
LLAT	h=100	50	267	2001.5	65.25*	466.5*
		75	441	1244.25	110.25*	280*
	h=150	50	699.25	1650.25	198.5*	470.5*
		75	698.5	1486	201.25*	382.25*
	h=155	50	622	1146	172.75	334.25
		75	600	1041.75	173	301.25

* There is a significant difference ($P < 0.05$) in the dose values between points at different heights for all projections except LLAT, for which in fluoroscopy mode, the difference of dose rate at heights of 100 and 150 cm was not significant ($P = 0.25$).

Table 2 shows the Organ Dose / DAP ratio in different organs of the cardiologist for actual angiography conditions. Vertical dose rate variations at the location of the cardiologist checked out with phantom and the results are shown in Table 3. Figure 6 shows the diagram of dose changes at the physician's location for two different imaging modes: Fluoroscopy and Cine. Dose values at the height of 100 cm for both fluoroscopic and Cine modes are $286.25 \pm 2.1 \mu\text{Gy} / \text{hour}$ and $1179.75 \pm 7.7 \mu\text{Gy} / \text{hour}$, respectively.

The results of dose rate measurements in 4 projections of LLAT, RLAT, LPO45 °, and RPO45 ° in two fluoroscopy and cine modes are given in Table 4. After analyzing the data, it was found that in both cine and fluoroscopy modes, there is a significant difference ($P = 0.05$) in the dose values between points at different heights for all projections except LLAT, for which in fluoroscopy mode, the difference of dose rate at heights of 100 and 150 cm was not significant ($P = 0.25$).

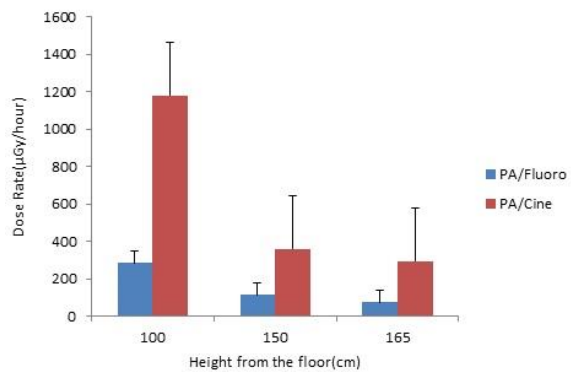


Figure 6. Absorbed dose rate at different heights at the physician's location

Discussion

The aim of this study was to investigate the distribution of the dose rate from scatter radiation in coronary angiography and to reduce the cumulative dose of people involved in this procedure. To reduce the dose, the principles of radiation protection, including using a lead cover, reducing the fluoroscopic time, and increasing the distance from the tube, are usually performed. Increasing the distance from the tube without disturbing the cardiologists' work is one of the most effective ways to reduce the dose to them. Dose

distribution information and identification of projections with less risk compared to high-risk projections could be helpful in regard to the selection of the best location for cardiologists and other personnel. In Table 5, the results of this study have been compared with several studies in fluoroscopic mode.

Results of these studies showed that the dose rate is reduced with increasing the height from the floor. It is worth noting that these values are collected in different devices with different radiation conditions. Our study was a single-center study, and the dose distribution was examined on a Siemens angiography device. Many factors such as kVp, mAs, functional mode, and automatic brightness control system influence the dose rate.[26,27] The operator function in setting the field size and adjusting the number of pulses per second and the width of the pulses has a significant effect on the dose rate. The impact of radiation pulses per second is so important that it alone can cause significant changes in the dose rate. In fact, by increasing the number of pulses per second, the dose of the patient's skin surface and consequently the dose of the scatter beam will increase[28,29]. The choice of the operator depends strictly on the quality of the image. This device had the ability to irradiate with the number of pulses of 10, 15, and 30 pulses per second. The ratio of the dose of the eye and thyroid organs has been considered in several articles. In this study, this ratio was calculated to be 0.65 for PA projection in fluoroscopic mode. This ratio varies between 0.5 to 0.75 in different studies [18]. Clerinex et al. used the Monte Carlo simulation to obtain the eyes to thyroid dose ratio of 0.75 [30]. This ratio is important because in this center, in almost all cases, physicians observed the use of lead protection to protect the thyroid (thyroid gland), while they did not wear the protective glasses (only two of the twelve physicians in this department wore lead glasses) while the dose rate around the eye is only 35% lower than the thyroid dose rate. By examining the changes in dose rate in the

direction of the bed in the PA projection, it can be claimed that by changing the location of the physician only about 20 cm from the previous location at distances less than 140 cm from the tube, there will be a significant decrease in dose rate in the waist area ($P = 0.01$). In fluoroscopy and cine modes, the physician's ratio of dose with this displacement is 0.73 and 0.7; respectively; compared to the previous condition. The use of this technique (increasing the distance from the tube) in fluoroscopic mode may disrupt the cardiologist's work due to the guidance of the catheter and guide wire, but in cine mode is very efficient because it creates no restrictions on the physician's movement.

Dose to DAP conversion coefficients can be used to express the risk of different projections for organs with different heights. This quantity is used as an efficient quantity in expressing the risk of each projection independent of radiation parameters (kVp, mA), field size, and patient thickness [31-33]. Comparison of the dose conversion coefficients to DAP indicates a significant difference ($P = 0.05$) between different projections. Due to the location of dosimetry points close to the direction of the main beam, the coefficient has the highest value for LPO45 ° projection, which indicates that this projection is high risk. In the case of RLAT projection, the proximity of the physician to the X-ray tube causes they receive more scattered X-ray photons from the collimator, and the dose rate in this area is in third place in terms of the amount of scatter radiation received by the physician.

The risk of RPO projection is also higher than the PA projection. The results of DAP values compared to other studies are shown in table 6.

Schultz et al. investigated the ratio of effective dose coefficient to DAP in both PA and LLAT projections using Monte Carlo simulation, and the value of effective dose conversion ratio to DAP in LLAT projection was 1.29 ± 0.16 times of the PA projection [31].

Table 5. The results of this study compared with several studies in fluoroscopic mode.

Study	height	165 cm from the floor (μGy/hour)	150 cm from the floor (μGy/hour)	100 cm from the floor (μGy/hour)
This study	2/1* ±76		115/25±1/7*	286/25±2/1*
Mesbahi [22]	90		140	200
Schueler [13]	--		400	1600
Ubeda [23]	140		--	290
Chida [24]	--		282± 187/2*	443±237*
Kuon [25]	70		100	155

*These values are the standard deviation of the mean.

Table 6. The results of DAP values compared to other studies

Study	Height	165 cm from the floor (μGy/Gy.cm ²)	150 cm from the floor (μGy/Gy.cm ²)	100 cm from the floor (μGy/Gy.cm ²)
This study	Fluoro	2.11±0.06*	3.21±0.05*	7.95±0.06*
	Cine	1.92±0.02*	2.36±0.02*	7.71±0.05*
Ferrira[19]	Fluoro	--	3.3	9.3
Schueler[13]	Fluoro	--	2.3	11

*These values are the standard deviation of the mean.

Koukorava et al. identified RLAT projection as the most risky projection, followed by RPO, LPO, LLAT, and PA, respectively [34]. Clouvas et al. expressed the risk between six different projections using Monte Carlo simulations, and the results of their study were similar to this study for four projections (all projections except LPO projection [35]. Kuon et al. compared different projections using Monte Carlo simulations. In terms of the physician's effective dose, the lowest dose was obtained for PA and LPO projections, and the highest dose rate was report for RLAT, RPO, and LLAT projections, respectively [25]. One of the limitations of our study is that it is done in one center on one device. It is suggested that measurements be performed in more centers and on more devices in future studies.

Conclusion

This study showed that increasing the distance by 20 cm from the tube at distances less than 140 cm can reduce the dose to the physicians by 37% - 43%. The dose for the eyes area is only 35% less than the dose for the thyroid area, and the use of lead glasses can significantly reduce the effective annual dose of the physician. Choosing the appropriate projection for coronary angiography can significantly reduce the dose for cardiologist, so using RLAT projection instead of LLAT projection can reduce the dose rate to different organs by 50%. Further studies should be conducted about the effect of different projections with the same clinical use about dose distribution in coronary angiography to provide the best working conditions for physicians and staff.

Acknowledgment

We would like to thank all those who helped and supported us in this research, including the Tehran University of Medical Sciences and the angiography department of Ayatollah Taleghani Hospital.

References

1. Mc Namara K, Alzubaidi H, Jackson JK. Cardiovascular disease as a leading cause of death: how are pharmacists getting involved?. *Integrated pharmacy research & practice*. 2019;8:1.
2. Tsao CW, Aday AW, Almarzooq ZI, Alonso A, Beaton AZ, Bittencourt MS, et al. Heart disease and stroke statistics—2022 update: a report from the American Heart Association. *Circulation*. 2022;145(8):e153-e639.
3. <https://www.who.int/news-room/fact-sheets/detail/the-top-10-causes-of-death>.
4. Tavakoli MB, Jabbari K, Jafari S, Hashemi SM, Akbari M. Evaluating the Absorbed Dose of Skin, Thyroid and Eye in Coronary Angiography CT Imaging and Its Comparison with Conventional Angiography. *Journal of Isfahan Medical School*. 2011;29(159).
5. Tavakoli H M, Jabari K, Salman J. SU-E-I-51: Investigation of Absorbed Dose to the Skin, Eyes and Thyroid of Patients during CT Angiography and Comparison with Conventional Angiography. *Medical physics*. 2012;39(6Part4):3636.
6. Kočka V. The coronary angiography—An old-timer in great shape. *Cor et vasa*. 2015;57(6):e419-e24.
7. Tavakoli MB, Faraji R, Sajjadih A, Jafari S. Determination of the weighted computed tomography dose index in coronary multidetector computed tomography angiography. *Journal of Isfahan Medical School*. 2016 Oct 22;34(398):1060-5.
8. Afzalipour R, Abdollahi H, Hajjalizadeh M, Jafari S, Mahdavi SR. Estimation of diagnostic reference levels for children computed tomography: A study in Tehran, Iran. *International Journal of Radiation Research*. 2019;17(3):407-13.
9. Jafari S, Ghazikhanlu Sani K, Karimi M, Khosravi H, Goodarzi R, Pourkaveh M. Establishment of Diagnostic Reference Levels for Computed Tomography Scanning in Hamadan. *Journal of Biomedical Physics & Engineering*. 2020;10(6):792.
10. Schiefer R, Rickli H, Neurauter E, Buser M, Weilenmann D, Maeder MT. Non-invasive assessment prior to invasive coronary angiography in routine clinical practice in Switzerland—Is it according to the guidelines?. *Plos one*. 2019 Sep 6;14(9):e0222137.
11. Williams MC, Stewart C, Weir NW, Newby DE. Using radiation safely in cardiology: what imagers need to know. *Heart*. 2019;105(10):798-806.
12. Roh Y, Kim J, Park H, Kim J, Ryu D, Chun K, et al. Effect of Exposure Angulation on the Occupational Radiation Exposure during Cardiac Angiography: Simulation Study. *International Journal of Environmental Research and Public Health*. 2021;18(15):8097.
13. Schueler BA, Vrieze TJ, Bjarnason H, Stanson AW. An investigation of operator exposure in interventional radiology. *Radiographics*. 2006;26(5):1533-41.
14. Mesbahi A, Aslanabadi N, Mehnati P, Keshtkar A. Evaluation of Patients' Exposure during Angiography and Angioplasty Procedures in the Angiography Department of Shahid Madani Hospital in Tabriz. *Iranian Journal of Medical Physics*. 2009;6(1):53-9.
15. Chida K, Inaba Y, Saito H, Ishibashi T, Takahashi S, Kohzuki M, et al. Radiation dose of interventional radiology system using a flat-panel detector. *American Journal of Roentgenology*. 2009;193(6):1680-5.
16. Aichinger H, Dierker J, Joite-Barfuß S, Säbel M. Image Receptors. In *Radiation Exposure and Image Quality in X-Ray Diagnostic Radiology*. 2012;67-83.
17. Mohammadi M, Danaee L, Alizadeh E. Reduction of radiation risk to interventional cardiologists and patients during angiography and coronary angioplasty. *The Journal of Tehran University Heart Center*. 2017;12(3):101.
18. Martin C. A review of radiology staff doses and dose monitoring requirements. *Radiation protection dosimetry*. 2009;136(3):140-57.
19. Ferrari P, Venturi G, Gualdrini G, Rossi P, Mariselli M, Zannoli R. Evaluation of the dose to the patient and medical staff in interventional cardiology employing computational models. *Radiation protection dosimetry*. 2010;141(1):82-5.

20. Schultz F, Zoetelief J. Dosemeter readings and effective dose to the cardiologist with protective clothing in a simulated interventional procedure. *Radiation protection dosimetry*. 2008;129(1-3):311-5.
21. Struelens L, Carinou E, Clairand I, Donadille L, Ginjaume M, Koukorava C, et al. Use of active personal dosimeters in interventional radiology and cardiology: Tests in hospitals—ORAMED project. *Radiation measurements*. 2011;46(11):1258-61.
22. Mesbahi A, Mehnati P, Keshtkar A, Aslanabadi N. Comparison of radiation dose to patient and staff for two interventional cardiology units: a phantom study. *Radiation protection dosimetry*. 2008;131(3):399-403.
23. Ubeda C, Vano E, Gonzalez L, Miranda P, Valenzuela E, Leyton F, et al. Scatter and staff dose levels in paediatric interventional cardiology: a multicentre study. *Radiation protection dosimetry*. 2010;140(1):67-74.
24. Chida K, Morishima Y, Inaba Y, Taura M, Ebata A, Takeda K, et al. Physician-received scatter radiation with angiography systems used for interventional radiology: comparison among many X-ray systems. *Radiation protection dosimetry*. 2012;149(4):410-6.
25. Kuon E, Empen K, Reuter G, Dahm JB. Höhe und Röhrenangulation als die Determinanten der möglichen Untersucher-Ortsdosisleistung in der invasiven Kardiologie. In *RöFo-Fortschritte auf dem Gebiet der Röntgenstrahlen und der bildgebenden Verfahren*. 2004;176: 739-45.
26. Fink GE. Radiation safety in fluoroscopy for neuraxial injections. *the official scholarly journal of the American Association of Nurse Anesthesiology*. 2009;77(4).
27. Wagner LK, Archer BR, Cohen AM. Management of patient skin dose in fluoroscopically guided interventional procedures. *Journal of Vascular and Interventional Radiology*. 2000;11(1):25-33.
28. Crowhurst J, Whitby M. Lowering fluoroscopy pulse rates to reduce radiation dose during cardiac procedures. *Wiley Online Library*. 2018; 247-9.
29. Pyne CT, Gadey G, Jeon C, Piemonte T, Waxman S, Resnic F. Effect of reduction of the pulse rates of fluoroscopy and CINE-acquisition on X-ray dose and angiographic image quality during invasive cardiovascular procedures. *Circulation: Cardiovascular Interventions*. 2014;7(4):441-6.
30. Clerinx P, Buls N, Bosmans H, De Mey J. Double-dosimetry algorithm for workers in interventional radiology. *Radiation protection dosimetry*. 2008;129(1-3):321-7.
31. Schultz F, Geleijns J, Spoelstra F, Zoetelief J. Monte Carlo calculations for assessment of radiation dose to patients with congenital heart defects and to staff during cardiac catheterizations. *The British journal of radiology*. 2003;76(909):638-47.
32. Heye S, Maleux G, Oyen RH, Claes K, Kuypers DR. Occupational radiation dose: percutaneous interventional procedures on hemodialysis arteriovenous fistulas and grafts. *Radiology*. 2012;264(1):278-84.
33. Lecomte J. Radon and the system of radiological protection. *Annals of the ICRP*. 2012;41(3-4):389-96.
34. Koukorava C, Carinou E, Ferrari P, Krim S, Struelens L. Study of the parameters affecting operator doses in interventional radiology using Monte Carlo simulations. *Radiation measurements*. 2011;46(11):1216-22.
35. Clouvas A, Xanthos S, Antonopoulos-Domis M, Silva J. Monte Carlo calculation of dose rate conversion factors for external exposure to photon emitters in soil. *Health physics*. 2000;78(3):295-302.